

THE DESIS L2A PROCESSOR AND VALIDATION OF L2A PRODUCTS USING AERONET AND RADCALNET DATA

R. de los Reyes¹, K. Alonso¹, M. Bachmann², E. Carmona¹, M. Langheinrich¹, R. Müller¹, B. Pflug³, and R. Richter¹

¹ German Aerospace Center (DLR), Earth Observation Center, Remote Sensing Technology Institute, Oberpfaffenhofen, Wessling, Germany

² German Aerospace Center (DLR), Earth Observation Center, Remote Sensing Data Center, Oberpfaffenhofen, Wessling, Germany

³ German Aerospace Center (DLR), Earth Observation Center, Remote Sensing Technology Institute, Berlin-Adlershof, Germany

Commission I, WG I/1

KEY WORDS: DESIS, surface reflectance, L2A, aerosols, water vapor, hyperspectral

ABSTRACT:

The hyperspectral instrument "DLR Earth Sensing Imaging Spectrometer" (DEGIS) is a VNIR sensor on-board of the International Space Station (ISS) and operational since October 2019. DESIS acquires images of Earth on user request with a swath of about 30 km width and 235 bands with a Full Width at Half Maximum (FWHM) of 3.5 nm in the spectral range between 400 to 1000 nm.

In this article we will present the basis of the atmospheric correction by PACO software, implemented inside the DESIS Ground Segment as L2A processor. The resulting L2A products will be validated against independent in-situ measurements.

The aerosol optical thickness and water vapor will be compared with the Aerosol Robotic Network (AERONET) measurements and the surface reflectance will be validated with the Radiometric Calibration Network (RadCalNet) data.

1. INTRODUCTION

The DESIS L2A processor corrects the terrestrial reflection of the incident solar radiation from the effect of the atmospheric constituents. On its way down to the Earth surface and up towards the DESIS sensor, the solar radiation is affected by different absorption and scattering processes. The spatial and temporal variation in composition and properties of some of these constituents makes the compensation of atmospheric effects an important step in the remote sensing applications to retrieve consistent surface properties (Vermote et al., 1997) (Thompson et al., 2018) (Franch et al., 2017).

This contribution will summarize the DESIS L2A products (Section 2) and their validation using in-situ measurements (Sections 3.1 and 3.2). The conclusions (Section 4) will summarize the estimation of the uncertainty in the surface reflectance.

2. DESIS L2A PROCESSOR AND PRODUCTS

Within the DESIS Ground Segment, the PACO software (de los Reyes et al., 2020) is implemented as L2A processor. The algorithms implemented in PACO are inherited from ATCOR (Richter, 1998).

The L2A processing is based on the following procedures. As a first step, *Look-Up-Tables* (LUTs) with *radiative transfer* (RT) functions have been simulated using MODTRAN 5.4.0 (Berk, 2008) for both mid-latitude summer and winter atmospheres. The aerosol type in the simulations corresponds to the MODTRAN rural (i.e. continental). The simulated radiative transfer functions are transformed to sensor radiative transfer LUTs, convolving them with the DESIS spectral response function per band. The same spectral response functions are used to calculate the solar irradiance for the specific sensor using a pre-selected solar model with the standard setting using in Fontenla (Fontenla et al., 2011).

Based on L1C ortho-rectified images, the following processing steps are called by the processor in order to produce the corresponding L2A products (Section 2.1):

- Pre-classification of the scene pixels according to pre-defined categories: land, water, clouds, shadows, haze, Dark Dense Vegetation (DDV), etc.
- Estimation of the atmospheric visibility and Aerosol Optical Thickness (AOT) per pixel, extracting the information from the previously masked DDV pixels. If no DDV pixels are identified, a default visibility of 23 km is assumed for pixels in the scene (Kaufman et al., 1997) (Richter et al., 2006).
- Calculation of the Water Vapor (WV) column map using the Atmospheric Pre-corrected Differential Absorption algorithm (Schläpfer et al., 1998) (Richter and Schlapfer, 2008) using the 820 nm absorption region. The WV is calculated only for land pixels. For water pixels, the reflected signal is so low that the WV estimation algorithm retrieve only noise. Therefore, the mean over land pixels is assumed for the water pixels.
- Calculation of the rugged-terrain or flat-terrain atmospheric correction per pixel, without any Bi-directional reflectance correction, resulting in a Lambertian surface reflectance.

2.1 L2A products

The DESIS L2A products are included in the following data layers, which are provided to the user:

- Pre-classification mask (*QL_QUALITY-2*): pixel mask of coded 8-bit integer flag, following the criteria and the flagging criteria detailed in (Alonso et al., 2019) (de los Reyes et al., 2020).

- Aerosol optical thickness map (*QL_QUALITY - 2*): estimated AOT at 550 nm (dimensionless) per pixel.
- Water vapor column map (*QL_QUALITY - 2*): estimated water vapor column (in cm).
- BOA surface reflectance (*SPECTRAL_IMAGE*): surface reflectance (without BRDF correction) measured in "percent (%) * 100".

3. VALIDATION OF DESIS L2A PRODUCTS AND UNCERTAINTY ESTIMATION

The validation of the DESIS products is presented in this section. Note that there are no independent references data available for the pre-classification masks, therefore they are excluded from this validation study.

The validation of the L2A products is divided according to the in-situ reference sources: AERONET stations (Holben et al., 1998) for the atmospheric parameters AOT and WV (Section 3.1) and RadCalNet (Bouvet et al., 2019) for the surface reflectance (Section 3.2). As DESIS is not a mapping mission, the number of available acquisitions over the reference sites depend on the users requests and their priority. For this reason, the statistics available for the products evaluation are limited in some cases.

Nevertheless, this study will determine the uncertainty (de los Reyes et al., 2020) over the full dataset available of the AOT, WV and the surface reflectance estimation. The uncertainty propagation or uncertainty for different acquisition conditions is out of this current study.

3.1 Validation of atmospheric parameters: aerosols and water vapor

The aerosol optical thickness and water vapor column products are validated using the measurements of the AERONET sun-photometers as reference.

The AERONET stations measure at different times, so the values within ± 30 min of the DESIS acquisitions are interpolated to the DESIS acquisition time. The AOT is measured at different wavelengths by the AERONET station, so an additional interpolation in wavelengths to 550 nm must be included in our analysis. The standard deviation of the interpolating values plus an instrumental 10% uncertainty is considered in the AERONET measurement error.

The final interpolated values of AOT and WV are compared with the value derived from DESIS in a ROI (Region Of Interest) of 9 km diameter on the AOT (550 nm) and WV maps around the AERONET station coordinates.

For the AOT, only the DESIS acquisitions with enough detected DDVs ($>5\%$) in the scene are considered for this study. This data quality criteria is set to exclude from the study the scenes where the default AOT values is used, and not the AOT estimation algorithm.

Finally, a total of 47 scenes were included to determine the AOT uncertainty. Unfortunately not enough scenes have an AOT > 0.2 (see Figure 1), as a result few bins with enough data are available to calculate an uncertainty as a function of the reference AERONET AOT. For the total amount of the scenes available for this study, we obtain an RMSE ~ 0.15 .

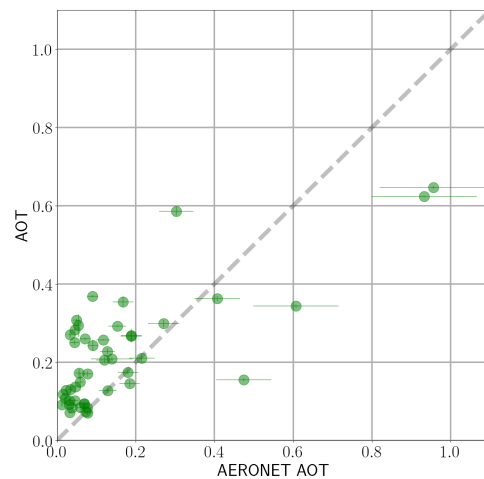


Figure 1. DESIS versus AERONET AOT (550 nm) (green dots). The 1:1 line is represented by a grey dashed lines.

Regarding the WV evaluation, only scenes with enough ($>5\%$) clean land pixels will be considered. A total of 141 scenes along the full range of values is available (see Figure 2). The calculated uncertainty of the water product of DESIS L2A products between 0. and 5. cm is $U_{WV} = (0.08 \pm 0.02) \cdot WV(cm) + (0.06 \pm 0.03)cm$.

This uncertainty results are better than those obtained by PACO in Sentinel-2 multi-spectral study (de los Reyes et al., 2020). The reason is likely the higher spectra resolution and therefore the smaller spectral difference between the absorption and the shoulders bands for hyperspectral data compared to multispectral like Sentinel-2.

For DESIS, due to the etaloning effect for higher wavelengths (> 800 nm) (Alonso et al., 2019), it is not possible to evaluate analytically whether the improvement in water vapor comes from the hyperspectral sensor or the difference in the water vapor absorption bands.

3.2 Validation of Bottom-Of-Atmosphere products: surface reflectance

The Bottom-Of-Atmosphere is validated with the in-situ measurements at the RadCalNet sites. Each of the site has an homogeneity uncertainty (U) within an specific ROI (Table 1). In order to calculate a surface reflectance mean over the highest amount of pixels possible, the minimum ROI of interest to consider should include at least 5x5 pixels (150 x 150 m).

RadCalNet	U [%]	ROI [m]
La Crau	5	500
Gobabeb	3	500
Railroad Valley Playa	1.5	1000

Table 1. RadCalNet sites with their corresponding ROI and uncertainty for this study.

In order to compare with previous studies on multi-spectral sensors like Sentinel-2 (de los Reyes et al., 2020) and to minimize Bi-directional reflection (BRD) effects, illumination conditions of sun zenith angle $< 30^\circ$ and off-nadir tilt angle $< 10^\circ$ are only considered.

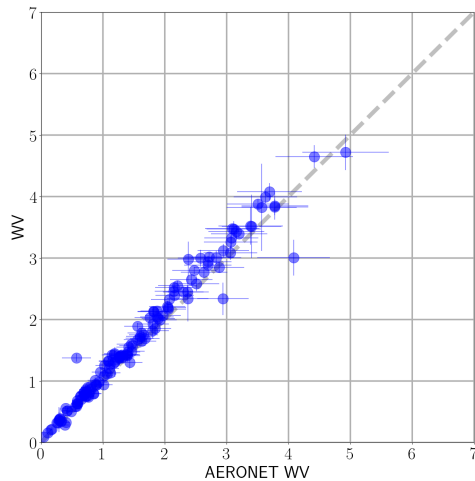


Figure 2. DESIS versus AERONET water vapor (in cm) (blue dots). The 1:1 line is represented by a grey dashed lines.

The accuracy, the precision and the uncertainty are calculated in this study only for scenes over Gobabeb site (see Figure 3, where at east 7 scenes are available under the before mentioned illumination conditions).

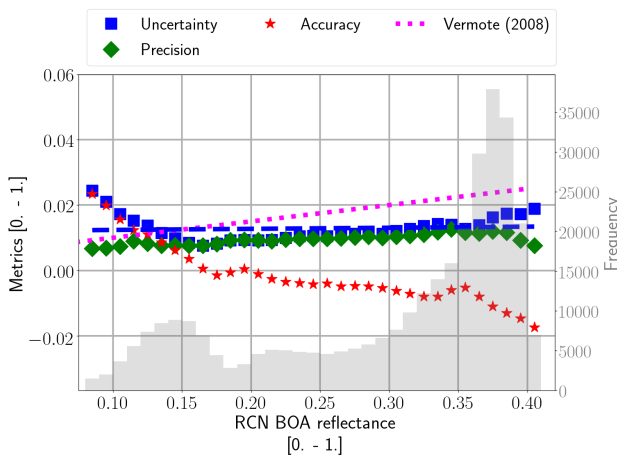


Figure 3. Accuracy (red star), precision (green diamond) and uncertainty (blue square) as a function of the reference value of DESIS surface reflectance for Gobabeb RadCalNet site. The number of pixels included in each bin are shown in the shadow histogram and in the right axis. Uncertainty fit is displayed as dotted blue line.

The dashed blue line is the resulting linear fit to the uncertainty curve, $U_{BOA} = (0.04 \pm 0.02) \cdot \rho_{BOA} + (0.011 \pm 0.006)$.

The large offset (0.011 ± 0.006) compared with Landsat-8 reference value (0.005) (Vermote and Kotchenova, 2008) plotted as pink dashed line (Figure 3) is due to the accuracy bias at low frequencies ($\lambda < 440nm$).

Next section will demonstrate that this accuracy bias seems to be due to the large uncertainty in the AOT estimation in this type of scenes. For such arid scenes a default value of between 0.2 - 0.3 is used in comparison with the typical values of RadCalNet acquisitions ($AOT < 0.1$).

3.2.1 L2AF: L2A surface reflectance with external AOT measurements In order to demonstrate the effect of the AOT estimation on the uncertainty, the measured value of the AOT during the RadCalNet measurement is used during the atmospheric correction of DESIS scene. The external AOT values can be given as input during the atmospheric correction in the PACO software branch (de los Reyes et al., 2020) implemented as DESIS L2A processor. The aerosol type is the same as in DESIS ("rura") and the same used in RadCalNet for the calculation of TOA reflectances. The AOT "forced" surface reflectance is named L2AF in this study, and its uncertainty results are shown in Figure 4. The resulting uncertainty of $U_{BOA_{L2AF}} = (0.014 \pm 0.002) \cdot \rho_{L2AF} (0.005 \pm 0.000)$ shows an agreement with the precision and proves the previous assumption that the accuracy bias at short wavelengths is due to a large AOT uncertainty.

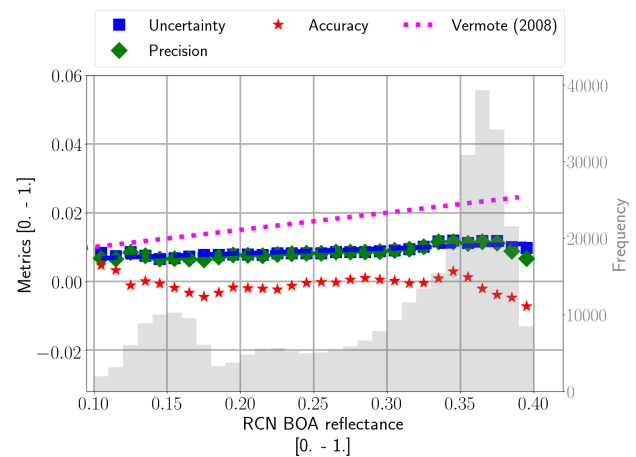


Figure 4. Accuracy (red star), precision (green diamond) and uncertainty (blue square) as a function of the reference value of DESIS surface reflectance for Gobabeb RadCalNet site. The number of pixels included in each bin are shown in the shadow histogram and in the right axis. Uncertainty fit is displayed as dotted blue line.

3.2.2 BOA reflectance: DESIS versus RadCalNet at La Crau Once we have estimated the surface reflectance uncertainty in the worst conditions (large AOT uncertainty), we will apply these results to a La Crau scene acquired at sun zenith angles $< 30^\circ$ and off-nadir $< 10^\circ$.

Figure 5 shows the DESIS and RadCalNet spectra assuming the uncertainties given in Section 3.2 and Table 1. The DESIS and RadCalNet data corresponds to June 20th, 2020. The coverage factor (k) of the difference between both spectra is within the combined uncertainty ($k < 1$). The error source of both measurements are considered independent and added quadratically to calculate the combined uncertainty. The only outlier correspond to the first DESIS band, and is related to known manufacturing defects of the DESIS detector at position of La Crau site for this scene in particular (close to the tile border).

4. CONCLUSIONS

After three years of operations of the DESIS sensor, enough data is available to give an estimation of the uncertainty of the DESIS products.

An uncertainty of $(0.08 \pm 0.02) \cdot WV(cm) + (0.06 \pm 0.03)cm$ has been estimated when comparing the water vapor estimated

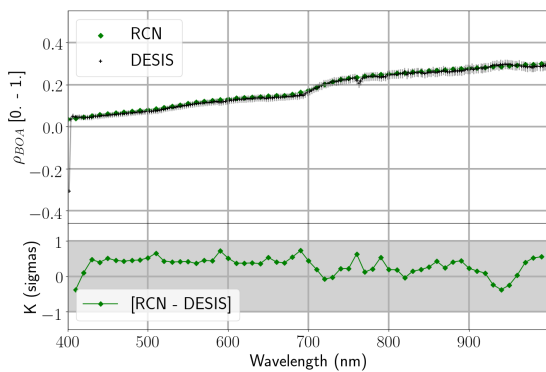


Figure 5. Top: DESIS surface reflectance (black cross) and RadCalNet (green diamond) in-situ measurement for La Crau (France) on June 20th, 2020. Bottom: Residuals of the difference between the spectra above.

by DESIS to the AERONET in-situ measurements used as reference.

An estimation of the DESIS surface reflectance product uncertainty is calculated using the in-situ measurements of the RadCalNet sites. Under low sun zenith angle and small off-nadir geometry, the uncertainty of the DESIS surface reflectance is $(0.04 \pm 0.02) \cdot \rho_{BOA} + (0.011 \pm 0.006)$ for wavelengths $\lambda > 440$ nm. For lower wavelengths, the AOT uncertainty is dominant over the fitted curve, being up to 0.02 - 0.03 surface reflectance (where 1 corresponds to 100%) for the blue wavelengths when the AOT difference is of the order of a factor 10.

Finally, when used the estimated uncertainties in this study with an scene with dark dense vegetation, the comparison between the DESIS BOA and the in-situ measurements are within their corresponding errors.

REFERENCES

Alonso, K., Bachmann, M., Burch, K., Carmona, E., Cerra, D., de los Reyes, R., Dietrich, D., Heiden, U., Hölderlin, A., Ickes, J., Knodt, U., Krutz, D., Lester, H., Müller, R., Pagnutti, M., Reinartz, P., Richter, R., Ryan, R., Sebastian, I., Tegler, M., 2019. Data Products, Quality and Validation of the DLR Earth Sensing Imaging Spectrometer (DESI). *Sensors*, 19(20).

Berk, A., 2008. MODTRAN 5.2.0 user's manual.

Bouvet, M., Thome, K., Berthelot, B., Bialek, A., Czaplak-Myers, J., Fox, N. P., Goryl, P., Henry, P., Ma, L., Marcq, S., Meygret, A., Wenny, B. N., Woolliams, E. R., 2019. RadCalNet: A Radiometric Calibration Network for Earth Observing Imagers Operating in the Visible to Shortwave Infrared Spectral Range. *Remote Sensing*, 11(20).

de los Reyes, R., Langheinrich, M., Schwind, P., Richter, R., Pflug, B., Bachmann, M., Müller, R., Carmona, E., Zekoll, V., Reinartz, P., 2020. PACO: Python-Based Atmospheric Correction. *Sensors*, 20(5).

Fontenla, J. M., Harder, J., Livingston, W., Snow, M., Woods, T., 2011. High-resolution solar spectral irradiance from extreme ultraviolet to far infrared. *Journal of Geophysical Research: Atmospheres*, 116(D20).

Franch, B., Vermote, E., Roger, J.-C., Murphy, E., Becker-Reshef, I., Justice, C., Claverie, M., Nagol, J., Csiszar, I., Meyer, D., Frederic, B., Ed, M., Wolfe, R., Devadiga, S., Csiszar@noaa, I., Gov, Moreno, J., Atzberger, C., Thenkabail, P., 2017. A 30+ Year AVHRR Land Surface Reflectance Climate Data Record and Its Application to Wheat Yield Monitoring. *Remote Sensing*, 9.

Holben, B., Eck, T., Slutsker, I., Tanré, D., Buis, J., Setzer, A., Vermote, E., Reagan, J., Kaufman, Y., Nakajima, T., Lavenu, F., Jankowiak, I., Smirnov, A., 1998. AERONET—A Federated Instrument Network and Data Archive for Aerosol Characterization. *Remote Sensing of Environment*, 66(1), 1 - 16.

Kaufman, Y. J., Wald, A. E., Remer, L., Gao, B.-C., Li, R.-R., Flynn, L., 1997. The MODIS 2.1- μ m channel-correlation with visible reflectance for use in remote sensing of aerosol. *IEEE Trans. Geoscience and Remote Sensing*, 35, 1286-1298.

Richter, R., 1998. Correction of satellite imagery over mountainous terrain. *Appl. Opt.*, 37(18), 4004-4015.

Richter, R., Schlapfer, D., 2008. Considerations on Water Vapor and Surface Reflectance Retrievals for a Spaceborne Imaging Spectrometer. *IEEE Transactions on Geoscience and Remote Sensing*, 46(7), 1958-1966.

Richter, R., Schläpfer, D., Müller, A., 2006. An automatic atmospheric correction algorithm for visible/NIR imagery. *International Journal of Remote Sensing*, 27, 2077-2085.

Schläpfer, D., Borel, C. C., Keller, J., Itten, K. I., 1998. Atmospheric Precorrected Differential Absorption Technique to Retrieve Columnar Water Vapor. *Remote Sensing of Environment*, 65(3), 353 - 366.

Thompson, D., Guanter, L., Berk, A., Gao, B.-C., Richter, R., Schläpfer, D., Thome, K., 2018. Retrieval of Atmospheric Parameters and Surface Reflectance from Visible and Shortwave Infrared Imaging Spectroscopy Data. *Surveys in Geophysics*, 39.

Vermote, E. F., El Saleous, N., Justice, C. O., Kaufman, Y. J., Privette, J. L., Remer, L., Roger, J. C., Tanré, D., 1997. Atmospheric correction of visible to middle-infrared EOS-MODIS data over land surfaces: Background, operational algorithm and validation. *Journal of Geophysical Research: Atmospheres*, 102(D14), 17131-17141.

Vermote, E. F., Kotchenova, S., 2008. Atmospheric correction for the monitoring of land surfaces. *Journal of Geophysical Research: Atmospheres*, 113(D23).